

1 **An experimental study of the solubility and speciation of**
2 **tantalum in fluoride-bearing aqueous solutions at elevated**
3 **temperature**

4
5 TIMOFEEV, A.¹, ART.A. MIGDISOV² AND A.E. WILLIAMS-JONES

6
7 Department of Earth & Planetary Sciences, McGill University, 3450 University Street, Montreal, QC,
8 Canada, H3A 0E8.

9 ¹alexander.timofeev@mail.mcgill.ca

10 ²Earth and Environmental Division, Los Alamos National Laboratory, P.O. Box 1663, M.S. J535, Los
11 Alamos, NM 87545, U.S.A.

Abstract

41
42
43 The solubility of Ta₂O₅ (solid) and the speciation of tantalum in HF-bearing aqueous solutions have
44 been determined at temperatures of 100-250 °C and vapour-saturated water pressure. Tantalum is
45 transported as the species Ta(OH)₅⁰ at low HF concentration and pH ~1-3. At higher HF concentration,
46 tantalum mobility is controlled by the species TaF₃(OH)₃⁻ and TaF₅⁰; the presence of TaF₅⁰ is only evident
47 at ≤150 °C. Equilibrium constants range from -17.4 ± 0.45 to -16.4 ± 0.12 for the formation of Ta(OH)₅⁰
48 from crystalline Ta₂O₅ and from -8.24 ± 0.64 to -8.55 ± 0.68 for the formation of TaF₃(OH)₃⁻ at 100 and
49 250 °C, respectively. For TaF₅⁰, they were determined to be 0.13 at 100 °C and -0.35 at 150 °C.

50 In many respects, the behaviour of tantalum in acidic fluoride-bearing solutions is similar to that
51 of niobium. The solubility of Ta₂O₅ (solid) is not dependent on HF concentration in fluoride-poor fluids,
52 but rises rapidly at higher HF concentration. However, at the conditions of our experiments, namely a
53 pH of ~2, temperature up to 250 °C, and a wide range of HF concentrations, Ta₂O₅ (solid) solubility is
54 almost invariably lower than that of Nb₂O₅ (solid). Modelling of Nb and Ta leaching confirmed the
55 preferential mobility of niobium under most conditions expected in natural fluoride-rich hydrothermal
56 systems. This modelling also demonstrated that both niobium and tantalum are rapidly deposited upon
57 removal of fluoride from an acidic brine. As a result of hydrothermal alteration, the Nb/Ta ratios of
58 secondary minerals may increase relative to those of the primary mineral, or remain largely unaffected,
59 depending on the pH of the fluid.

60

61 1. Introduction

62 Niobium and tantalum are considered geochemical twins, the aqueous behaviour of which is
63 governed by their high charge (5+) and small radius (Pearson, 1963). Although they are immobile in
64 most hydrothermal systems, reports of parts per million concentrations of niobium in fluid inclusions
65 indicates that under some conditions at least, niobium may be mobilised hydrothermally (Rickers et al.,

66 2006). Further evidence of such mobility is provided by the Nechalacho alkaline igneous intrusion, in
67 which the niobium and tantalum mineralisation, with rare exception, has a hydrothermal origin
68 (Timofeev and Williams-Jones, 2015). Alkaline igneous systems of this kind, which contain appreciable
69 concentrations of niobium and tantalum, are typically associated with fluoride alteration (e.g., Sheard et
70 al., 2012). Insights into the conditions under which niobium is mobile were provided recently by the
71 experimental study of Timofeev et al. (2015). This study investigated the solubility of Nb₂O₅ (solid) in
72 fluoride-bearing solutions and showed that the stability of niobium species increases exponentially with
73 increasing HF concentration in the fluid. The study also emphasised the importance of acidity in
74 promoting the mobility of niobium.

75 Because of the similarity of tantalum to niobium, the solubility and speciation of tantalum is
76 predicted to be similar to that of niobium. Like Nb⁵⁺, Ta⁵⁺ is a hard acid and should form strong
77 complexes with the hard base, F⁻ (Pearson, 1963; Williams-Jones and Migdisov 2014). The first indication
78 that tantalum might behave differently from niobium in hydrothermal solutions was provided by
79 Zaraisky et al. (2010) who found that dissolution of columbite-(Mn) in a HF-bearing hydrothermal fluid
80 at 400 °C and 100 Mpa yielded a concentration of tantalum that was an order of magnitude less than
81 that of niobium. However, the results of these experiments are difficult to interpret because of the
82 chemically complex nature of the solid and the lack of constraints placed on their experimental solution;
83 the pH of the experimental solution and the stability constants of aqueous niobium and tantalum
84 species were not evaluated. Nonetheless, their results indicate that the behaviour of tantalum in
85 hydrothermal fluids may not mirror that of niobium, which is contrary to the conclusion of some studies
86 of natural systems that the mobility of niobium and tantalum is roughly equal (e.g., Lumpkin and Ewing,
87 1992; Novák and Černý, 1998). They are also consistent with evidence from polyoxometalate studies
88 that niobate and tantalate behaviour differs for some species, notably the hexaniobate and hexatantalate
89 ions (Fullmer et al., 2014).

90 In this paper, we report the results of experiments conducted at 100, 150, 200, and 250 °C, and
91 vapor-saturated water pressure designed to determine the solubility of Ta₂O₅ (solid). The experiments
92 were conducted at pH values of ~1 to 3 and HF concentrations from 10⁻⁵ to 10⁰ mol/kg. Results of these
93 experiments are used to evaluate the speciation of tantalum at the conditions of interest, and
94 determine formation constants for the dominant species. In conjunction with the results of Timofeev et
95 al. (2015) on niobium solubility and speciation, we evaluate the potential of an ore-forming fluid to
96 transport tantalum and niobium under hydrothermal conditions. We then evaluate the likelihood that
97 differences in tantalum and niobium speciation will control the Nb/Ta ratios of secondary minerals.

98

99

2. Methods

100 2.1 Experimental technique

101 The experiments involved measuring the solubility of synthetic Ta₂O₅ (solid) (99.99%, Alfa Aesar)
102 in aqueous solutions of variable pH and HF concentration at temperatures of 100, 150, 200, and 250 °C,
103 and vapor-saturated water pressure. The pH at the temperatures of interest ranged from 0.8 to 3.2, with
104 most experiments being carried out at a pH of ~2.0; the HF concentration ranged from 10⁻⁵ to 10⁰
105 mol/kg. Experiments were performed in Teflon test tubes contained within titanium autoclaves (Fig. 1).
106 Overall, the methodology employed in the experiments is similar to that of Migdisov and Williams-Jones
107 (2007). The reader is therefore directed to this paper for information not covered in the text that
108 follows.

109 Fluoride concentration was controlled by dissolving known amounts of NaF in nano-pure water.
110 The pH of each solution was then reduced to the level of interest by adding an appropriate amount of
111 trace metal grade HClO₄. In order to maintain the predominance of ClO₄⁻, a non-complexing ligand, over
112 HF as the background electrolyte, an amount of NaClO₄ approximately equal to that of NaF was added
113 to each experimental solution containing more than 10⁻² m NaF. Experiments were initiated by placing

114 small sealed Teflon holders containing Ta₂O₅ powder in Teflon test tubes, to which 20 ml of
115 experimental solution was added. The Teflon test tubes were then placed in titanium autoclaves
116 containing water (or solutions identical in composition to that used in the experiment) in order to
117 balance pressures developed inside and outside the test tube, and heated in a Fisher Isotemp forced
118 draft oven to the temperature of interest.

119 The time required to reach equilibrium was determined from a series of experiments of variable
120 duration performed at 100 °C and 0.075 mol/kg HF. The duration of the experiments ranged from 1 to 9
121 days, with a steady state concentration, assumed to represent equilibrium, being reached after 6 days
122 (Fig. 2). On the basis of the results from these kinetic experiments, all subsequent experiments were
123 conducted for durations greater than six days. Heating, quenching and sampling of the autoclaves were
124 carried out in less than an hour to minimize Ta₂O₅ (solid) dissolution and precipitation before or after an
125 experiment, respectively.

126 Following completion of an experiment, the autoclave was quenched in cold water and the Ta₂O₅-
127 bearing Teflon holder within the larger Teflon test tube was removed. The Ta₂O₅ (solid) within the Teflon
128 holder was analyzed by X-ray diffraction after completion of the experiments. No additional solids were
129 detected, though we cannot entirely exclude the possibility of trace amounts of a solid tantalum fluoride
130 phase being present in the experiments. A small aliquot of liquid (2 ml) was extracted from the Teflon
131 test tube in order to measure the pH and fluoride concentration of the experimental solution. The pH
132 (25 °C) of the latter was determined potentiometrically using a glass pH electrode. The acidity of the
133 aliquot of experimental solution was then neutralized by adding 2 ml of TISAB II (Deionized water >84%,
134 Sodium Acetate 8%, Sodium Chloride 6%, Acetic Acid 1%, CDTA <1%, Supplier: Thermo Fisher Scientific)
135 solution and the fluoride concentration was measured using a Thermo Scientific Orion fluoride ion
136 selective electrode. After removal of the above aliquot of liquid, one milliliter of TM grade HF was added
137 to the Teflon test tube in order to dissolve any tantalum that may have precipitated on its walls during

138 quenching. The concentration of tantalum from the resulting solutions was measured using ICP-MS
139 (UQAM, Montreal).

140 Of potential concern for the interpretation of the results of the experiments is the decomposition
141 of perchlorate at the elevated temperature of the experiments. It is unlikely, however, that the effect of
142 perchlorate decomposition was more than the experimental error of our experiments for the following
143 reasons. 1) If perchlorate decomposition had significantly affected the results of our experiments, there
144 would have been a steady deviation with time in the tantalum concentration determined in our kinetic
145 runs from the equilibrium concentration. This was not the case. 2) Similar experiments performed in
146 perchlorate-based solutions at the same temperatures to investigate the speciation of rare-earth
147 elements and zirconium were not affected by the decomposition of perchlorate (Migdisov and Williams-
148 Jones, 2007; Migdisov et al., 2009, 2011).

149

150

3. Results

151 3.1 Identification of dissolved tantalum species

152 The results of the experiments performed at 100 to 250 °C, which are reported in Table 1, were
153 used to identify the dissolved tantalum species. Two distinct trends are present in the data for all
154 temperatures investigated (Fig. 3). At high HF activity, the logarithm of tantalum activity has a slope of
155 ~3 with respect to the logarithm of HF activity. In addition, experiments performed at different pH
156 conditions indicate that at 200 and 250 °C the logarithm of tantalum activity increases with increasing
157 pH in the proportion 1:1 (Fig. 4c-d). The only tantalum species which can satisfy both of these
158 relationships via its formation reaction is $\text{TaF}_3(\text{OH})_3^-$, which forms as follows:



160 At lower temperature, 100 and 150 °C, the dependence of the increase in the logarithm of
161 tantalum activity with increasing pH decreases and approaches the proportion of ~1/2 at 100 °C (Fig. 4a-

162 b). Moreover, the slope in the logarithm of Ta activity versus HF activity at these temperatures exceeds
 163 3 (Fig. 3a-b). By analogy with the Zr-bearing fluoride system within which species such as $Zr(OH)_3F^0$ and
 164 $Zr(OH)_2F_2^0$ predominate at $>150\text{ }^\circ\text{C}$, but ZrF_5^- and ZrF_6^{2-} become increasingly abundant at $<150\text{ }^\circ\text{C}$ (Aja et
 165 al., 1995; Migdisov et al., 2011), we propose that this reflects the presence of a simple tantalum fluoride
 166 species, namely TaF_5^0 , at lower temperature and pH:



168 The stability of this species is not pH dependent. As such, the slope of $\sim 1/2$ in Ta-pH space
 169 represents the transition with decreasing pH from the predominance of $TaF_3(OH)_3^-$, having a Ta-pH slope
 170 of 1, to the predominance of TaF_5^0 , having a Ta-pH slope of 0. The predicted tantalum activity calculated
 171 using the formation constants for reactions (1), (2), (3) that are derived later show this gradual
 172 transition, and are in good agreement with our experimental data (Fig. 4). In addition, the expected
 173 slope relating changes in TaF_5^0 activity to increasing HF activity is 5 ($10HF^0:2TaF_5^0 \rightarrow 5:1$). This explains the
 174 increase in slope that we observe in the logarithm of tantalum activity with respect to HF activity at 100
 175 and $150\text{ }^\circ\text{C}$; TaF_5^0 becomes increasingly more abundant at higher HF activity at these temperatures (Fig.
 176 3).

177 The trends in the data are strikingly different at lower HF concentration. The activity of tantalum
 178 is unaffected by HF activity at all temperatures, nor is it affected by the pH of the solution (Fig. 3, Fig. 5).
 179 These observations, coupled with the identification of niobium hydroxide species by Timofeev et al.
 180 (2015) at similar conditions, lead us to conclude that the predominant tantalum species at these lower
 181 HF concentrations is $Ta(OH)_5^0$:



183 In order to calculate equilibrium constants for reactions (1), (2), and (3), it was necessary to use
 184 an activity model. The model used to calculate the activity of the dissolved species is presented in the
 185 next section and is the same as that used to determine the pH for each experiment.

186

187 3.2 Methods used in calculating ion activity

188 To calculate the activity of the ions, we used the extended Debye-Hückel equation (Helgeson et
189 al., 1981):

$$190 \log \gamma_n = -\frac{A \cdot [z_n]^2 \cdot \sqrt{I}}{1 + B \cdot \hat{a} \cdot \sqrt{I}} + b_\gamma \cdot I \quad (4)$$

191 with A and B being the parameters of the Debye-Hückel equation, b_γ the extended parameter, which
192 depends on the nature of the background electrolyte, \hat{a} the distance of closest approach, which is
193 specific to the ion of interest, z the charge of the ion, and I the true ionic strength when all dissolved
194 components are considered. The values of b_γ , the extended parameter, were taken from Migdisov and
195 Williams-Jones (2007), who determined the best fit b_γ values for ClO_4^- in a chemically similar system. The
196 distances of closest approach (\hat{a}), were set at 9 Å for H^+ (Kielland, 1937; Garrels and Christ, 1965), 3.5 Å
197 for F^- and OH^- (Garrels and Christ 1965), 4 Å for Na^+ (Garrels and Christ, 1965) and at 4.5 Å for ClO_4^- and
198 $\text{TaF}_3(\text{OH})_3^-$. In order to calculate pH at the conditions of interest, it was assumed that HClO_4 dissociates
199 completely. The pH and activity of the dissolved species were refined iteratively for each experiment
200 considering the following species: H^+/OH^- , Na^+ , HF^0 , ClO_4^- , $\text{Ta}(\text{OH})_5^0$, TaF_5^0 , $\text{TaF}_3(\text{OH})_3^-$. The Haar-
201 Gallagher-Kell (Kestin et al., 1984) and Marshall and Franck (1981) models were used to determine the
202 thermodynamic properties and dissociation constant of H_2O under our experimental conditions.
203 Thermodynamic data for the aqueous species were obtained from Ryzhenko (1965), Ryzhenko et al.
204 (1991), Johnson et al. (1992), Sverjensky et al. (1997), and Shock et al. (1997). With this activity model in
205 hand, it was possible to calculate the equilibrium constants of reactions (1), (2) and (3).

206

207 3.3. Derivation of stability constants

208 The results of the experiments given in Table 1 were used to calculate equilibrium constants for
209 the reactions presented in Equations (1), (2), and (3) by iteratively minimizing the error function U,
210 which is given by the expression:

$$211 \quad U = \sum_i \left(\frac{\log C_{\text{Ta}}^{\text{Theo}} - \log C_{\text{Ta}}^{\text{Exp}}}{\log C_{\text{Ta}}^{\text{Exp}}} \right)^2 \quad (5)$$

212 where i is the i th experimental point in the dataset, $C_{\text{Ta}}^{\text{Exp}}$ is the concentration of Ta determined
213 experimentally, and $C_{\text{Ta}}^{\text{Theo}}$ is the concentration of Ta calculated theoretically using the starting
214 compositions, the activity model, and the values of the formation constants, which were adjustable
215 parameters in these iterations. The modeled system involved the same species as those considered in
216 the calculation of ion activity. The error function, U, was minimized iteratively using the Nelder-Mead
217 simplex search algorithm (Nelder and Mead, 1965; Dennis and Woods, 1987) for isothermal sets of
218 solutions with the activity coefficients of the species and ionic strength recalculated after each iteration.
219 Additional details on the methods of minimization can be found in Migdisov and Williams-Jones (2007)
220 and Migdisov et al. (2009), which used the same data treatment method. The resulting equilibrium
221 constants are reported in Table 2. Equilibrium constant uncertainties were calculated by propagating the
222 error (1σ) associated with tantalum species activity, normalized to the same HF concentration, using
223 reactions (1), (2), and (3), and are also reported in Table 2. Uncertainties for the equilibrium constants
224 associated with the species, TaF₅ (Reaction 2), are not provided as the data were only sufficient to
225 permit approximate values for these equilibrium constants to be determined.

226

227 **4. Discussion**

228 **4.1 Comparison to previous studies**

229 Results of previous studies that are directly comparable to the data presented in this paper are
230 limited to those reported in the study of Zraisky et al. (2010). In their experiments Zraisky et al. (2010)

231 employed two starting solids; Ta₂O₅ of greater than 99.99% purity, and a single crystal of columbite-
232 tantalite from a quartz-amazonite-mica pegmatite. Whereas the solubility of Ta₂O₅ (solid) determined by
233 Zaraisky et al. (2010) can be compared easily to that reported in this study, the activity of tantalum
234 oxide within the columbite-(Mn) sample is uncertain and cannot be evaluated. Fortunately, electron
235 microprobe analyses of this crystal suggest that it is relatively homogeneous. Thus, although the
236 absolute solubility of the columbite-(Mn) may be difficult to interpret, relationships such as the change
237 in solubility of the columbite-(Mn) with an increase in HF activity should be consistent with this study, at
238 similar experimental conditions.

239 Two experiments were conducted by Zaraisky et al. (2010) at HF concentrations ranging from 0.01
240 to ~1 molal HF. The first at 400 °C used columbite-(Mn) as the solid, and the second at 550 °C employed
241 Ta₂O₅ (solid). A pressure of 100 Mpa and a Co-CoO oxygen buffer were employed in both experiments. It
242 was assumed that the solution descriptions of Zaraisky et al. (2010) were complete despite their lack of
243 detail. A 0.1 molal HF solution was therefore considered to have been prepared by the addition of an
244 appropriate amount of trace metal grade hydrofluoric acid to nanopure water. Using these
245 compositions, we calculated the pH and HF activity of each solution at the respective temperatures of
246 the two experiments. We then assumed that the tantalum species, TaF₃(OH)₃⁻, identified at higher HF
247 concentrations in this study is also stable at the higher temperature and pH (~4) conditions of the
248 experiments conducted by Zaraisky et al. (2010). The concentrations of tantalum in solution determined
249 by Zaraisky et al. (2010) were accordingly adjusted to a pH of 2.0 using the stoichiometry of reaction (1).
250 The results of these calculations are shown in Figure 6. A strong dependence of tantalum solubility with
251 increasing HF concentration is observed at both 400 and 550 °C. The slope of ~3 of this dependence is
252 identical to that observed by us at 100-250 °C, and would be the predicted slope, if our previous
253 assumption about TaF₃(OH)₃⁻ being the dominant tantalum species at higher temperature is correct. In
254 addition, the lower solubility of a tantalum solid at high temperature is consistent with the trends in the

255 stability of $\text{TaF}_3(\text{OH})_3^-$ determined in this study. The concentration of $\text{TaF}_3(\text{OH})_3^-$ reaches a maximum at
256 $\sim 150^\circ\text{C}$, i.e., the concentration of this species is lower at higher and lower temperature (Table 2, Fig. 7).
257 Therefore, consistent with this trend, the concentration of dissolved tantalum in equilibrium with
258 columbite-(Mn) at 400°C should be less than that predicted by the best fit to our data for 250°C , which
259 is what we observe (Fig. 6). If we extrapolate the results of this study to 400°C , the curve of best fit for
260 this temperature lies just above and parallel to the data of Zraisky et al. (2010). This constitutes a
261 remarkably high level of agreement, particularly considering that our study and that of Zraisky et al.
262 (2010) employed different solids for this temperature.

263 At the lowest HF concentration considered by Zraisky et al. (2010), 0.01 m HF, at 550°C , the
264 solubility of Ta_2O_5 (solid) is higher than would be expected solely from the presence of $\text{TaF}_3(\text{OH})_3^-$. This
265 could be due to the transition to the predominance field of $\text{Ta}(\text{OH})_5^0$, which we predict to be increasingly
266 stable at elevated temperature.

267

268 **4.2 Differences in the behaviour of tantalum and niobium**

269 Tantalum-bearing minerals, such as the columbite and pyrochlore group minerals, commonly
270 contain appreciable quantities of niobium. Therefore, a scenario favourable for the transport of
271 tantalum, such as the interaction of an acidic fluoride-bearing solution at elevated temperature with a
272 tantalum-bearing rock, might also be favorable for the transport of niobium. After this interaction,
273 however, the relative proportions of niobium and tantalum in the rock might have changed significantly.
274 The results of this study and those for niobium in similarly acidic, fluoride-bearing solutions reported by
275 Timofeev et al. (2015) allow us to assess the relative behaviour of these two metals during fluid-rock
276 interaction.

277 At low HF activity ($< \sim 10^{-3}$) and a pH of 2, the solubility Nb_2O_5 (solid) is independent of HF activity
278 but at higher HF activity the logarithm of the solubility of Nb_2O_5 (solid) increases at a rate of

279 approximately twice that of the logarithm of HF activity (Timofeev et al., 2015). By contrast, the
280 solubility of Ta₂O₅ (solid) is lower and begins rising at a much higher HF activity (10⁻²). The rate of
281 increase in the solubility of Ta₂O₅ (solid) with increasing HF activity, however, is higher, i.e., the
282 logarithm of aTa/aHF is ~3 (Fig. 7). If the data for niobium are extended to higher HF activity, it can be
283 seen that, despite the greater rate of increase in the solubility of Ta₂O₅ (solid) with increasing HF activity,
284 Ta₂O₅ (solid) solubility does not exceed that for Nb₂O₅ (solid) until a HF activity of ~0.25 or concentration
285 of ~5,000 ppm is reached. Although such a high fluoride concentration has been reported for a natural
286 system (Banks et al., 1994, reported HF concentrations for hypersaline fluids in the Capitan Pluton, New
287 Mexico, USA, ranging between ~500-5000 ppm), HF concentrations in most naturally occurring fluids are
288 likely to be significantly lower; they are buffered to low values by the precipitation of very weakly
289 soluble minerals, such as fluorite and topaz.

290 In order to evaluate the effect of an acidic, fluoride-bearing solution on a niobium- and tantalum-
291 bearing host rock, we modelled the progressive flushing of 50 grams of host rock containing 25 grams
292 each of Nb₂O₅ and Ta₂O₅ with a brine containing 50, 500, or 5000 ppm HF in addition to 1.5m NaCl, 0.5m
293 KCl, and 0.01m HCl, at 150 °C. The niobium and tantalum oxides were chosen due to the absence of
294 thermodynamic data for niobium and tantalum minerals. Their thermodynamic data were obtained
295 from Jacob et al. (2010) and Jacob et al. (2009), respectively. It should be noted that separate minerals
296 may control the relative solubility of niobium and tantalum in natural systems, thereby making the use
297 of niobium and tantalum oxides in the model a necessary, but potentially important simplification.
298 Thermodynamic data for the other minerals were obtained from Holland and Powell (1998) and Robie
299 and Hemingway (1995). Thermodynamic data for the aqueous species not considered in this study were
300 obtained from Johnson et al. (1992), Shock et al. (1997), Sverjensky et al. (1997), and Timofeev et al.
301 (2015). Extended parameters for NaCl in the Debye-Hückel equation were taken from Oelkers and
302 Helgeson (1991).

303 The results of this model are shown in Figure 8. The quantity of brine (containing 50 ppm HF)
304 needed to leach significant niobium from the original host rock exceeds a million liters. After interaction
305 of this amount of fluid with the rock, the content of tantalum was effectively unchanged. Increasing the
306 HF concentration to 500 ppm resulted in a two orders of magnitude reduction in the amount of brine
307 necessary to remove significant niobium. However, tantalum is difficult to mobilize, and approximately
308 one and a half order of magnitude more solution was required to leach tantalum in a proportion similar
309 to that of niobium. In our most HF-rich example, a brine containing 5,000 ppm HF is able to efficiently
310 leach both niobium and tantalum after interacting with less than a thousand liters of brine.
311 Nevertheless, more niobium is mobilized than tantalum in this fluoride-rich solution, albeit by a small
312 margin.

313 It should be noted that the data for tantalum collected in this study was to a higher HF activity
314 ($\log a_{\text{HF}} \sim -0.4$) than that for niobium ($\log a_{\text{HF}} \sim -2$) collected by Timofeev et al. (2015). Thus, it is
315 plausible that at higher HF activity than considered by Timofeev et al. (2015), the dependence of
316 niobium solubility on HF activity increases from a logarithmic slope of 2 to a slope of 3. Such an increase
317 is suggested by the observation that concentrations of niobium and tantalum in equilibrium with
318 columbite-(Mn) at 400 °C have similar dependencies on HF activity (Zaraisky et al., 2010). If the
319 logarithm of the slope of Nb solubility over HF activity were to approach that for tantalum at high HF
320 activity, transport of niobium would predominate relative to that of tantalum under almost any fluoride
321 activity at acidic conditions. However, Zaraisky et al. (2010) recognised a logarithmic molal Nb/HF slope
322 of 2 for their columbite-(Mn) solubility data, which is consistent with the neutral $\text{NbF}_2(\text{OH})_3^0$ species
323 identified by Timofeev et al. (2015). In order to achieve a logarithmic slope of 3, a pH dependence
324 similar to that suggested for the species $\text{TaF}_3(\text{OH})_3^-$ in this study would have to be present for a
325 negatively charged niobium hydroxyl-fluoride species.

326 If previously collected niobium speciation data are accurate to higher fluoride activity, pH could
327 play an important role in niobium-tantalum fractionation. The species, $\text{TaF}_3(\text{OH})_3^-$, is more stable at a
328 higher pH, whereas the stability of $\text{NbF}_2(\text{OH})_3^0$ is pH-independent (Timofeev et al., 2015). Therefore, the
329 HF activity at which tantalum species are more abundant than their niobium counterparts would
330 decrease considerably at elevated pH (e.g., 3-4 versus the value of ~ 2 employed in this study). During
331 fluid-rock interaction, however, although interaction of an acidic fluid with a calcium-bearing rock will
332 lead to an increase in its pH, the associated precipitation of fluorite and decrease in HF activity will result
333 in the deposition of Ta_2O_5 (solid) (Fig. 9). Thus, despite a delay in the deposition of Ta_2O_5 relative to
334 Nb_2O_5 because of the increase in pH, niobium species will remain more abundant in solution until the
335 concentration of all niobium and tantalum species fall below that of $\text{Ta}(\text{OH})_5^0$, the stability of which is
336 independent of pH and HF activity.

337

338 **4.3 Applications to natural systems**

339 Niobium-tantalum fractionation can occur not only during hydrothermal alteration of a host rock,
340 but also during subsequent events that result in the precipitation of niobium-tantalum bearing minerals.
341 To assess this latter possibility, we modelled two scenarios identical to those used by Timofeev et al.
342 (2015) to evaluate the hydrothermal deposition of niobium in natural systems. Both scenarios were
343 evaluated at 150 °C and saturated water pressure. In the first scenario, one liter of an acidic ($\sim \text{pH } 2.1$)
344 fluid with 500 ppm HF, 1.5m NaCl, 0.5m KCl, and 0.01m HCl, which was saturated with respect to Nb_2O_5
345 (solid) and Ta_2O_5 (solid), was mixed iteratively with 1mL aliquots of a brine containing 0.75m NaCl,
346 0.25m KCl, and 1m CaCl_2 until a 1:1 fluid ratio was reached (Fig. 9a). The starting concentration of HF
347 corresponds to that measured in fluid inclusions in the Capitan Pluton (Banks et al., 1994). In the second
348 scenario, an acidic fluid identical to that used in the first model was reacted iteratively with 10 mg
349 aliquots of calcite, representing a limestone or marble, until one liter of acidic solution had reacted with

350 2 grams of calcite (Fig. 9b). Thermodynamic data for the minerals and aqueous species involved in this
351 model are identical to those employed for the previous model addressing Nb₂O₅ and Ta₂O₅ dissolution.

352 By incorporating the data of this study, these models demonstrate the behaviour of tantalum
353 relative to niobium. Increases in pH in the first fluid mixing scenario are relatively minor and as such,
354 although concentrations of NbF₂(OH)₃⁰ and TaF₃(OH)₃⁻ decrease with progressive mixing and fluorite
355 deposition, both niobium and tantalum remain in solution. This decrease would be progressively
356 minimized with fluid mixing models incorporating lesser amount of calcium; fluorite would not
357 precipitate and most of the niobium and tantalum would remain in the fluid. By contrast, interaction of
358 the acidic brine with calcite (model 2) results in a large increase in pH, deposition of considerable
359 amounts of fluorite, and a rapid decrease in the concentration of the aqueous species of both niobium
360 and tantalum. From this perspective, the behaviour of niobium and tantalum appears to be quite similar
361 and the conclusions of Timofeev et al. (2015) validated; the neutralization of an acidic brine by
362 limestone or marble is a far more effective method for limiting the mobility of niobium and tantalum
363 than mixing with another brine. There is one notable difference in behaviour of the two metals in the
364 second model. As TaF₃(OH)₃⁻ is a pH-dependent species, the initially rapid rise in pH offsets the decrease
365 in HF activity caused by fluorite precipitation and results in an initial suppression of Ta₂O₅ (solid)
366 precipitation relative to that of Nb₂O₅ (solid). This interpretation is predicated on the assumption that
367 the niobium hydroxyl-fluoride species is neutrally charged. A negatively charged niobium hydroxyl-
368 fluoride species would eliminate this small depositional gap. However, this small difference is potentially
369 significant in interactions involving large amounts of fluid with wall rocks containing relatively minor
370 volumetric proportions of a Ca-bearing mineral (e.g., calcite). A hydrothermal fluid interacting with small
371 amounts of calcite would precipitate niobium-bearing minerals and in the process become progressively
372 enriched in tantalum relative to niobium. Further along the fluid pathway and following additional
373 neutralization, tantalum would be deposited. As a result, domains distinctly enriched in niobium and

374 tantalum may form upstream and downstream in the fluid conduit, respectively. Such domains would be
375 difficult to identify in natural environments, however, as the proportion of calcite required for such a
376 scenario has a very restricted range.

377 The results of the above models suggest that niobium and tantalum do not behave in an identical
378 fashion in hydrothermal fluids. If these two metals are leached from a host rock, a much lower fluid/rock
379 ratio is required to mobilize niobium than is the case for tantalum. Once the chemistry of the fluid is
380 altered such that the pH increases or HF activity decreases both niobium and tantalum precipitate. In
381 rare cases deposition of tantalum may be temporarily suppressed.

382 Niobium- and tantalum-bearing pegmatites that have experienced hydrothermal alteration
383 commonly demonstrate evidence of niobium and tantalum mobilization. For example, fine-grained
384 secondary muscovite containing ~50 ppm Ta and ~25 ppm Nb in the Tanco pegmatite is interpreted to
385 have crystallized from Ta-bearing aqueous fluids during a late hydrothermal event (Van Lichtenvelde et
386 al. 2008). In another example, Rickers et al. (2006) reported the occurrence of early fluid inclusions in
387 the Variscan Ehrenfriedersdorf complex that contain up to 29 ppm Nb; Ta was not analyzed.

388 Pegmatites that have been hydrothermally altered may retain their primary Nb/Ta ratios or have
389 quite different ratios of these metals. In the Moose II LCT (Li-Cs-Ta) pegmatite in the Northwest
390 Territories, Canada, the secondary muscovite is enriched in niobium and depleted in tantalum relative to
391 the primary muscovite (Anderson et al., 2013). Furthermore, overgrowths of columbite-(Fe) on primary
392 columbite-(Fe) crystals in the Moose II pegmatite are commonly Nb-rich. Based on these observations,
393 Anderson et al. (2013) concluded that the pegmatite had been enriched in Nb by a F- and Nb-rich fluid.
394 Indeed, the behaviour of Nb and Ta in this pegmatite is entirely consistent with the results of this study.
395 In other settings Nb/Ta ratios may remain largely unaffected by hydrothermal alteration. For example,
396 secondary tantalum oxide phases in the Moldanubicum granitic pegmatites, Czech Republic, have similar
397 Nb/Ta ratios to their primary counterparts (Novák and Černý, 1998). In the Tanco pegmatite, the Nb/Ta

398 ratios of the primary and secondary muscovite grains also do not differ greatly (Van Lichtenvelde et al.,
399 2008). Two factors may be responsible for Nb/Ta ratios remaining unaffected. The first is the pH of the
400 hydrothermal fluid. As mentioned previously, the solubility of tantalum in HF-rich systems increases
401 with increasing pH. Therefore, the Nb/Ta ratios of the secondary minerals could reflect the pH of the
402 altering hydrothermal fluid. Hydrothermal alteration of the Moose II pegmatite may have occurred at a
403 lower pH than the Tanco pegmatite, but this is not known as the pH of the altering fluid in these systems
404 was not constrained. Alternatively, the kinetics of Nb-Ta bearing mineral dissolution may be such that
405 the hydrothermal fluid does not achieve Nb-Ta saturation and the results of this study are not
406 applicable. However, kinetic runs performed in this study and by Timofeev et al. (2015) suggest that
407 Nb_2O_5 (solid) dissolution is faster than that of Ta_2O_5 (solid). As a result, we propose that pH, in addition
408 to HF activity, may play a role in determining the Nb/Ta ratios of secondary minerals.

409

410

5. Conclusions

411 The results of this study show that transport of tantalum in fluoride-bearing hydrothermal fluids is
412 controlled by $\text{Ta}(\text{OH})_5^0$ at low fluoride concentration, and $\text{TaF}_3(\text{OH})_3^-$ and TaF_5^0 , at high fluoride
413 concentration. Dissolved tantalum concentration rises rapidly at $>10^{-2}$ HF mol/kg. Niobium is more
414 soluble than tantalum in acidic hydrothermal fluids, except for those containing extremely high
415 concentrations of fluoride, explaining why niobium is commonly mobilized preferentially from niobium-
416 tantalum-bearing rocks. At higher pH, tantalum concentrations may approach those of niobium in
417 hydrothermal fluids, which could explain why Nb/Ta ratios of secondary minerals remain unchanged
418 from those of the primary minerals in some hydrothermally altered rocks.

419

420

Acknowledgements

421 This study was supported financially by NSERC CGM and FQRNT scholarships to A.T. and NSERC
422 Discovery and NSERC CRD grants to A.E.W.-J. The manuscript was improved significantly by comments
423 from three anonymous reviewers.

424 **References**

- 425 Aja S.U., Wood S.A. and Williams-Jones A.E. (1995) The aqueous geochemistry of Zr and the solubility of
426 some Zr-bearing minerals. *Appl. Geochem.* **10**, 603-620.
- 427 Anderson M.O., Lentz D.R., McFarlane C.R.M. and Falck H. (2013) A geological, geochemical and textural
428 study of a LCT pegmatite: implications for the magmatic versus metasomatic origin of Nb-Ta
429 mineralization in the Moose II pegmatite, Northwest Territories, Canada. *J. Geosci.* **58**, 299-320.
- 430 Banks D., Yardley B., Campbell A. and Jarvis K. (1994) REE composition of an aqueous magmatic fluid: a
431 fluid inclusion study from the Capitan Pluton, New Mexico, USA. *Chem. Geol.* **113**, 259–272.
- 432 Dennis Jr. J. E. and Woods D. J. (1987) Microcomputers in large-scale computing. In *New Computing*
433 *Environments* (ed. A. Wouk). SIAM, pp. 116-122.
- 434 Fullmer L.B., Molina P.I., Antonio M.R. and Nyman, M. (2014) Contrasting ion-association behaviour of
435 Ta and Nb polyoxometalates. *Dalton Trans.* **43**, 15295-15299.
- 436 Garrels R.M. and Christ C. L. (1965) *Solutions. Minerals. And Equilibria*. Harper & Row, New York.
- 437 Helgeson H. C., Kirkham D. H. and Flowers G. C. (1981) Theoretical prediction of the thermodynamic
438 behavior of aqueous electrolytes at high pressures and temperatures: IV. Calculation of activity
439 coefficients, osmotic coefficients, and apparent molal and standard and relative partial molal
440 properties to 600°. *Am. J. Sci.* **281**, 1249-1516.
- 441 Holland T. and Powell R. (1998) An internally consistent thermodynamic data set for phases of
442 petrological interest. *J. Metamorph. Geol.* **16**, 309-343.
- 443 Jacob K.T., Shekhar C. and Waseda Y. (2009) An update on the thermodynamics of Ta₂O₅. *J. Chem.*
444 *Thermodyn.* **41**, 748-753.
- 445 Jacob K. T., Shekhar C. and Vinay M. (2010) Thermodynamic properties of Niobium Oxides. *J. Chem. Eng.*
446 *Data* **55**, 4854-4863.
- 447 Johnson J. W., Oelkers E. H. and Helgeson H. C. (1992) SUPCRT92: a software package for calculating the
448 standard molal thermodynamic properties of minerals, gases, aqueous species, and reactions
449 from 1 to 5000 bar and 0 to 1000 °C. *Comput. Geosci.* **18**, 899-947.
- 450 Kestin J., Sengers J. and Kampgar-Parsi B. (1984) Thermo-physical properties of fluid H₂O. *J. Phys. Chem.*
451 *Ref.* **13**, 175-183.
- 452 Kielland J. (1937) Individual activity coefficients of ions in aqueous solutions. *J. Am. Chem. Soc.* **59**, 1675-
453 1678.
- 454 Lumpkin G.R., and Ewing, R.C. (1992) Geochemical alteration of pyrochlore group minerals: Microlite
455 subgroup. *Am. Mineral.* **77**, 179-188.
- 456 Marshall W. L. and Franck E. U. (1981) Ion product of water substance, 0-1000 °C, 1-10,000 bars. New
457 international formulation and its background. *J. Phys. Chem. Ref. Data* **10**(2), 295-304.
- 458 Migdisov A. A. and Williams-Jones A. E. (2007) An experimental study of the solubility and speciation of
459 neodymium (III) fluoride in F-bearing aqueous solutions. *Geochim. Cosmochim. Acta* **71**(12), 3056-
460 3069.
- 461 Migdisov A. A., Williams-Jones A. E. and Wagner T. (2009) An experimental study of the solubility and
462 speciation of the Rare Earth Elements (III) in fluoride- and chloride-bearing aqueous solutions at
463 temperatures up to 300 °C. *Geochim. Cosmochim. Acta* **73**, 7087-7109.

464 Migdisov A. A., Williams-Jones A. E., van Hinsberg V. and Salvi S. (2011) An experimental study of the
465 solubility of baddeleyite (ZrO₂) in fluoride-bearing solutions at elevated temperature. *Geochim.*
466 *Cosmochim. Acta* **75**(1), 7426-7434.

467 Nelder J. A. and Mead R. (1965) A simplex method for function minimization. *Comput. J.* **7**, 308-313.

468 Novák M. and Černý P. (1998) Niobium-tantalum oxide minerals from complex granitic pegmatites in the
469 Moldanubicum, Czech Republic: primary versus secondary compositional trends. *Can. Mineral.* **36**,
470 659-672.

471 Oelkers E. and Helgeson H. C. (1991) Calculation of activity coefficients and degrees of formation of
472 neutral ion pairs in supercritical electrolyte solutions. *Geochim. Cosmochim. Acta* **55**, 1235–1251.

473 Rickers K., Thomas R. and Heinrich W. (2006) The behaviour of trace elements during the chemical
474 evolution of the H₂O-, B-, and F-rich granite-pegmatite-hydrothermal system at
475 Ehrenfriedersdorf, Germany: a SXRF study of melt and fluid inclusions. *Miner. Deposita.* **41**, 229-
476 245.

477 Robie R.A. and Hemingway B.S. (1995) Thermodynamic properties of minerals and related substances at
478 298.15 K and 1 Bar (105 Pascals) pressure and at higher temperatures. *U.S. Geological Survey*
479 *Bulletin* 2131, 461pp.

480 Ryzhenko B. N. (1965) Determination of dissociation constant of hydrofluoric acid and conditions of
481 replacement of calcite by fluorite. *Geokhimiya* **3**, 273-276.

482 Ryzhenko B. N., Kovalenko N. I. And Mironenko M. V. (1991) Ionization-constant of hydrofluoric acid at
483 500 °C, 1kbar. *Dokl. Akad. Nauk SSSR* **317**, 203-206.

484 Sheard E. R., Williams-Jones A. E., Heiligmann M., Pederson C. and Trueman D.L. (2012) Controls on the
485 Concentration of Zirconium, Niobium, and the Rare Earth Elements in the Thor Lake Rare Metal
486 Deposit, Northwest Territories, Canada. *Econ. Geol.* **107**, p. 81-104.

487 Sverjensky D., Shock E. L. and Helgeson H. C. (1997) Prediction of the thermodynamic properties of
488 aqueous metal complexes to 1000 °C and 5kb. *Geochim. Cosmochim. Acta* **61**, 1359-1412.

489 Timofeev A., Migdisov A.A. and Williams-Jones A.E. (2015) An experimental study of the solubility and
490 speciation of niobium in fluoride-bearing aqueous solutions at elevated temperature. *Geochim.*
491 *Cosmochim. Acta* **158**, 103-111.

492 Timofeev A. and Williams-Jones A.E. (2015) The origin of niobium and tantalum mineralization in the
493 Nechalacho REE Deposit, NWT, Canada. *Econ. Geol.* **110**, 1719-1735.

494 Van Lichtenvelde M., Grégoire M., Linnen R.L., Béziat D. and Salvi S. (2008) Trace element geochemistry
495 by laser ablation ICP-MS of micas associated with Ta mineralization in the Tanco pegmatite,
496 Manitoba, Canada. *Contrib. Mineral. Petrol.* **155**, 791-806.

497 Williams-Jones A.E. and Migdisov A.A. (2014) Experimental constraints on the transport and deposition
498 of metals in ore-forming hydrothermal systems. *Society of Economic Geologist, Special Publication*
499 **18**, 77-95.

500 Wise M. A., Francis C. A. and Černý P. (2012) Compositional and structural variations in columbite-group
501 minerals from granitic pegmatites of the Brunswick and Oxford fields, Maine: Differential trends in
502 F-poor and F-rich environments. *Can. Mineral.* **50**, 1515-1530.

503 Zaraisky G. P., Korzhinskaya V. and Kotova N. (2010) Experimental studies of Ta₂O₅ and columbite-
504 tantalite solubility in fluoride solutions from 300 to 550°C and 50 to 100 MPa. *Miner. Petrol.* **99**,
505 287-300.

506

507 Table 1. Compositions of the experimental solutions (mol/kg).

T(°C)	ΣClO_4	$\text{Na}^+/\text{HF}^0, 10^{-2}$	Ta, 10^{-8}	pH (25 °C)	T(°C)	ΣClO_4	$\text{Na}^+/\text{HF}^0, 10^{-2}$	Ta, 10^{-8}	pH (25 °C)
100	0.036	1.20	1.81	1.67		0.028	0.0463	0.179	1.61
	0.024	0.572	0.47	1.78		0.059	0.0437	0.432	1.29
	0.0153	0.108	0.199	1.89		0.14	0.0414	0.183	0.92
	0.0149	0.0549	0.177	1.89		0.338	7.3	188	1.7
	0.0127	0.0103	0.138	1.94		0.27	7.65	314	1.95
	0.0127	0.00523	0.385	1.94		0.218	7.62	553	2.2
	0.0107	0.00158	0.144	2.01		0.191	7.71	938	2.4
	1.685	88.4	256000	2.7	150	0.207	7.56	1070	2.52
	1.28	75.5	209000	2.69	200	0.0303	0.915	1.10	1.72
	0.92	45.8	54500	2.66		0.0212	0.492	1.00	1.83
	0.37	19.8	8240	2.64		0.0149	0.0981	1.40	1.9
	0.151	8.22	418	2.55		0.0141	0.0613	1.13	1.91
	0.099	5.22	177	2.44		0.0108	0.0115	0.411	2.01
	0.0412	1.89	32.3	2.25		0.011	0.00753	0.665	2
	0.342	7.32	260	1.69		0.0107	0.00223	0.473	2.01
	0.266	7.47	382	1.96		1.35	54.4	449000	2.83
	0.218	7.69	449	2.2		1.02	48.3	399000	2.8
	0.19	7.56	591	2.4		0.828	36.7	133000	2.72
	0.208	7.53	726	2.51		0.362	19.1	22600	2.67
	0.165	7.56	1060	2.6		0.145	7.67	538	2.57
	0.207	7.44	693	2.51		0.0898	4.56	119	2.43
	0.207	7.47	674	2.51		0.0423	1.87	14.6	2.22
	0.208	7.56	798	2.51		0.00116	0.0549	0.495	3.08
100	0.029	1.04	2.02	1.77		0.00226	0.0494	0.425	2.74
150	0.0203	0.525	0.504	1.86		0.00515	0.0432	0.547	2.35
	0.013	0.0991	0.438	1.96		0.0104	0.052	0.856	2.04
	0.0125	0.0524	0.381	1.96		0.03	0.0419	0.617	1.64
	0.0105	0.00979	0.211	2.02		0.06	0.0369	0.639	1.29
	0.0102	0.00516	0.311	2.03		0.13	0.0355	0.434	0.94
	0.0102	0.00107	0.204	2.03		0.20	8.16	348	2.38
	0.0325	1.15	1.65	1.72		0.21	7.94	929	2.52
	0.0234	0.584	0.528	1.8		0.17	8.36	2150	2.59
	0.015	0.112	0.414	1.9	200	0.17	8.03	3770	2.64
	0.0132	0.0572	0.391	1.94	250	0.0332	1.05	0.546	1.69
	0.0116	0.0105	0.270	1.98		0.0252	0.60	1.08	1.76
	0.0124	0.00577	0.307	1.95		0.0173	0.132	0.618	1.84
	0.0115	0.00107	0.244	1.98		0.0167	0.0708	0.757	1.84
	0.873	42.4	208000	2.71		0.0128	0.0154	0.548	1.94
	0.358	18.0	18100	2.65		0.0119	0.0122	0.701	1.97
	0.122	6.07	784	2.71		0.0126	0.00506	0.680	1.94
	0.039	1.81	25.9	2.3		0.648	28.9	113000	2.68
	1.60	74.6	558000	2.69		0.541	24.2	64400	2.61
	1.16	59.3	448000	2.7		0.226	10.7	469	2.38
	0.87	37.9	207000	2.65		0.179	8.46	334	2.47
	0.35	16.8	20900	2.65		0.132	5.79	84.8	2.48
	0.14	7.03	759	2.55		0.0526	2.35	8.86	2.17
	0.09	4.31	209	2.46		0.295	8.92	54.2	1.9
	0.04	1.70	24.0	2.29		0.241	9.21	153	2.14
	0.00112	0.0481	0.186	3.08		0.208	8.71	240	2.33
	0.0024	0.0483	0.202	2.71		0.218	8.46	311	2.49
	0.0048	0.046	0.219	2.38	250	0.174	8.43	3060	2.61
	0.0104	0.0483	0.221	2.04					

508

509

510

511

512

513

514 Table 2: Equilibrium constants and their associated uncertainty for the Ta₂O₅ dissolution reactions, (1), (2), and (3).
 515
 516

T(°C)	100	150	200	250
Ta ₂ O ₅ ^{cryst} + 5H ₂ O = 2Ta(OH) ₅ ^o	-17.4 ± 0.45	-17.1 ± 0.32	-16.4 ± 0.36	-16.4 ± 0.12
Ta ₂ O ₅ ^{cryst} + 6HF ^o + H ₂ O = 2TaF ₃ (OH) ₃ ⁻ + 2H ⁺	-8.24 ± 0.64	-7.45 ± 0.65	-8.60 ± 0.64	-8.55 ± 0.68
Ta ₂ O ₅ ^{cryst} + 10HF ^o = 2TaF ₅ ^o + 5H ₂ O	~ 0.13	~ -0.35	-	-

517
 518
 519
 520
 521
 522
 523
 524
 525
 526
 527
 528
 529
 530
 531
 532
 533
 534
 535
 536
 537
 538
 539
 540
 541
 542
 543

544 Fig. 1. A schematic drawing illustrating the experimental set-up. *H₂O surrounding the Teflon test tube
545 was replaced by the experimental solution in a small number of experiments.
546

547 Fig. 2. Results from a series of experiments illustrating the solubility of Ta₂O₅ (solid) as a function of time
548 in an aqueous solution at 100 °C containing 0.075 mol/kg HF. The data suggest that equilibrium
549 (dashed line) was attained after 6 days.
550

551 Fig. 3. The solubility of Ta₂O₅ (solid), normalized to a pH of 2.0 on the basis of reactions (1), (2), and (3),
552 as a function of the concentration of HF at (a) 100 °C (b), 150 °C, (c), 200 °C, and (d) 250 °C. The
553 dashed lines indicate the solubility of Ta₂O₅ (solid) calculated from the values of log K for reactions
554 (1), (2), and (3) at each respective temperature. Results from the pH dependence experiments
555 illustrated in Figure 4 are also shown, but have not been normalized to a pH of 2. The results of
556 kinetic run experiments of duration of 6 days or more are included in the data set for 100 °C.
557

558 Fig. 4. The solubility of Ta₂O₅ (solid) as a function of pH at 100 °C (a), 150 °C (b), 200 °C (c), and 250 °C (d)
559 for solutions containing > 0.075 mol/kg HF. The dashed lines indicate the solubility of Ta₂O₅ (solid)
560 calculated from the values of log K for reactions (1), (2), and (3) at each respective temperature.
561

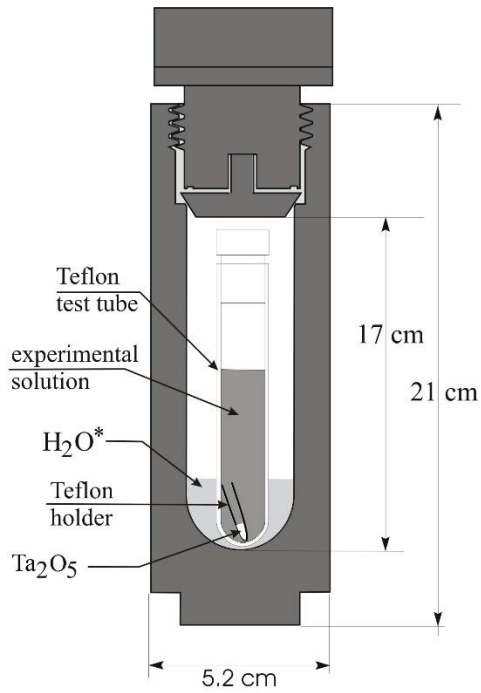
562 Fig. 5. The solubility of Ta₂O₅ (solid) as a function of pH at 150 and 200 °C in solutions containing ~5×10⁻⁴
563 mol/kg HF. The dashed lines represent best fits to the data calculated from the log K value of
564 reaction (1).
565

566 Fig. 6. Tantalum concentrations in equilibrium with columbite-(Mn) at 400 °C and Ta₂O₅ at 550 °C
567 calculated using data obtained by Zaraisky et al. (2010). The best fit of the solubility data obtained
568 at 250 °C in this study and extrapolated to 400 °C are shown for reference.
569

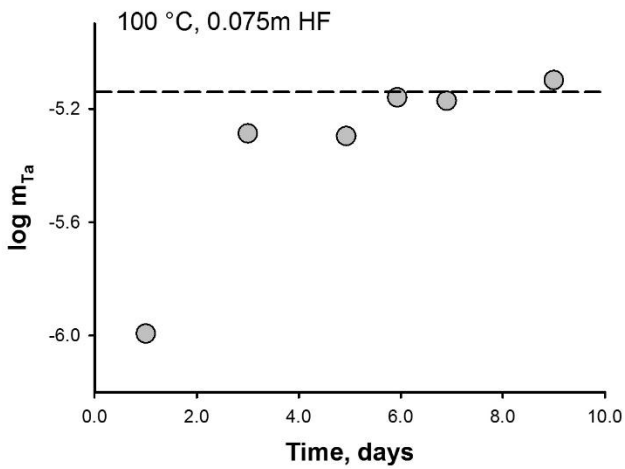
570 Fig. 7. The activity of Ta in equilibrium with Ta₂O₅ (solid) determined in this study at 100-250 °C
571 compared to the activity of Nb in equilibrium with Nb₂O₅ (solid) as determined by Timofeev et al.
572 (2015) at 150 °C.
573

574 Fig. 8. Amounts of Nb₂O₅ and Ta₂O₅ remaining from a sample initially containing 25 grams of each oxide
575 following progressive flushing of the sample with brine containing 50, 500, or 5000 ppm HF in
576 addition to 1.5m NaCl, 0.5m KCl, and 0.01m HCl, at 150 °C.
577

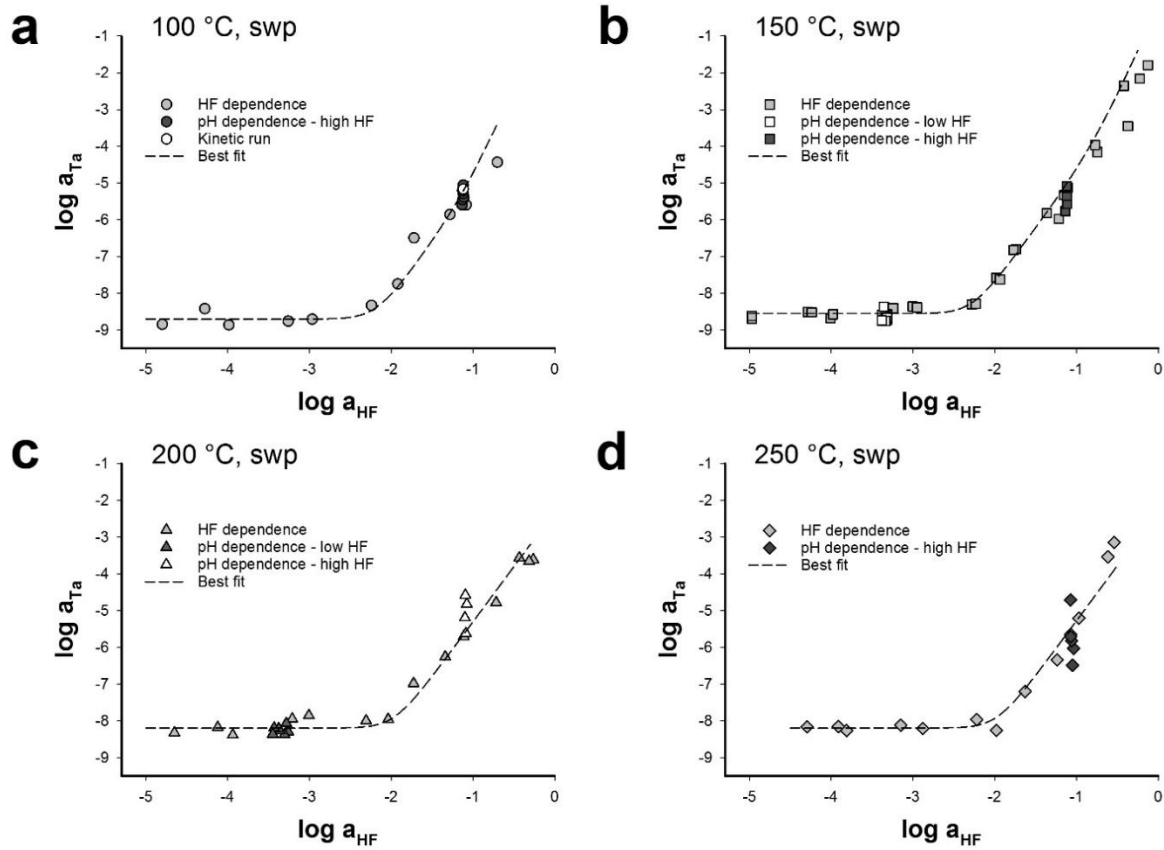
578 Fig. 9. The instantaneous concentrations of aqueous species and cumulative concentrations of
579 precipitated solids at 150 °C in a niobium- and tantalum-saturated fluid containing 500 ppm HF,
580 1.5m NaCl, 0.5m KCl, and 0.01m HCl (a) during progressive mixing with a brine containing 0.75m
581 NaCl, 0.25m KCl, and 1m CaCl₂, and (b) during progressive interaction with calcite (representing
582 limestone or marble).
583
584
585
586
587
588



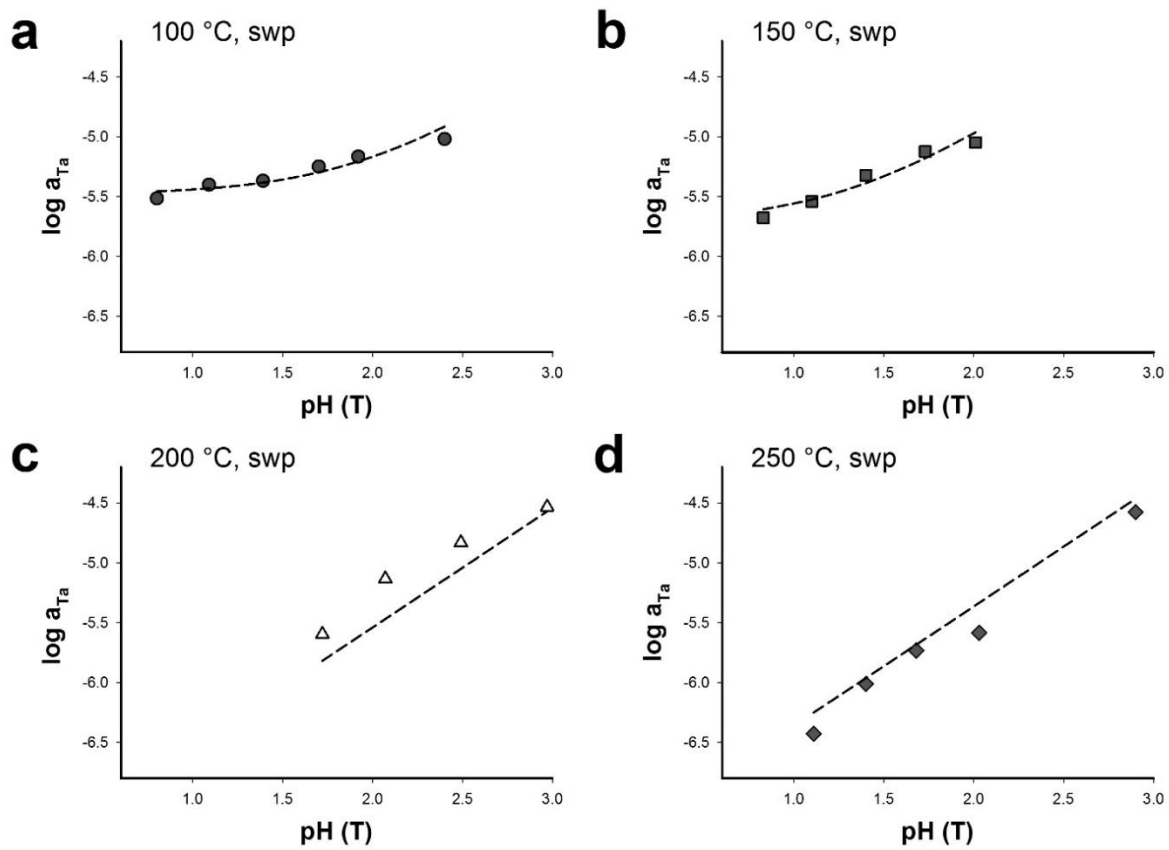
589
590
591 Figure 1
592



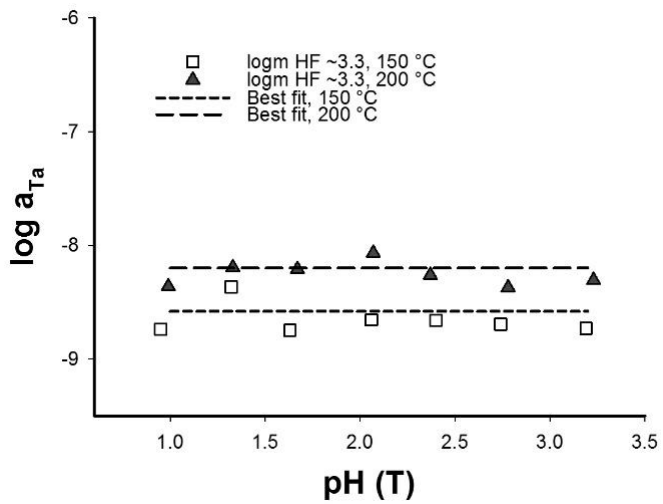
593
594 Figure 2
595



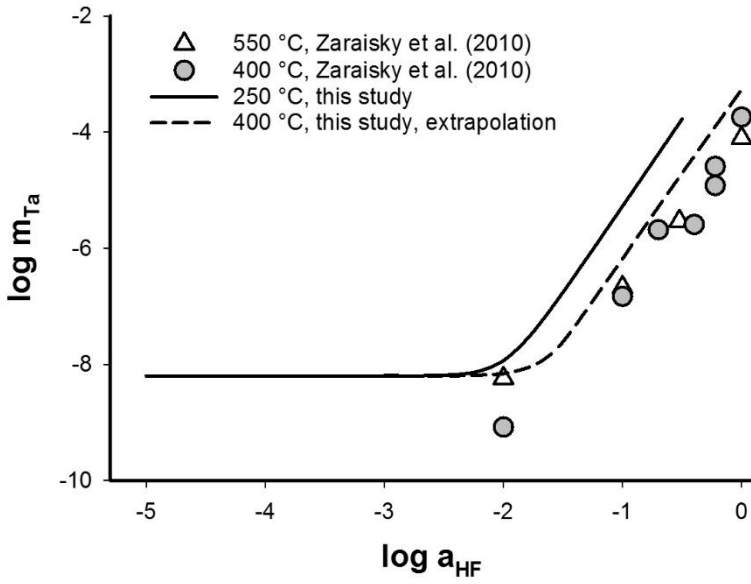
596
 597 Figure 3
 598
 599



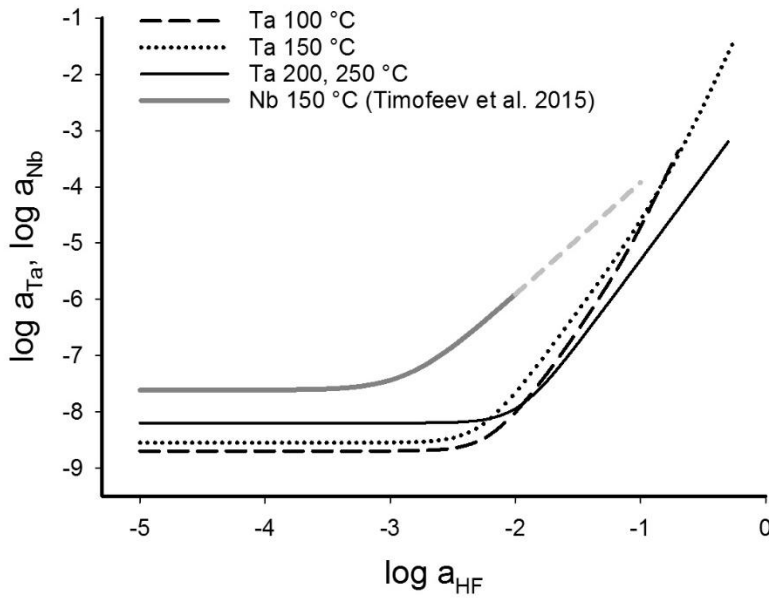
600
601 Figure 4
602



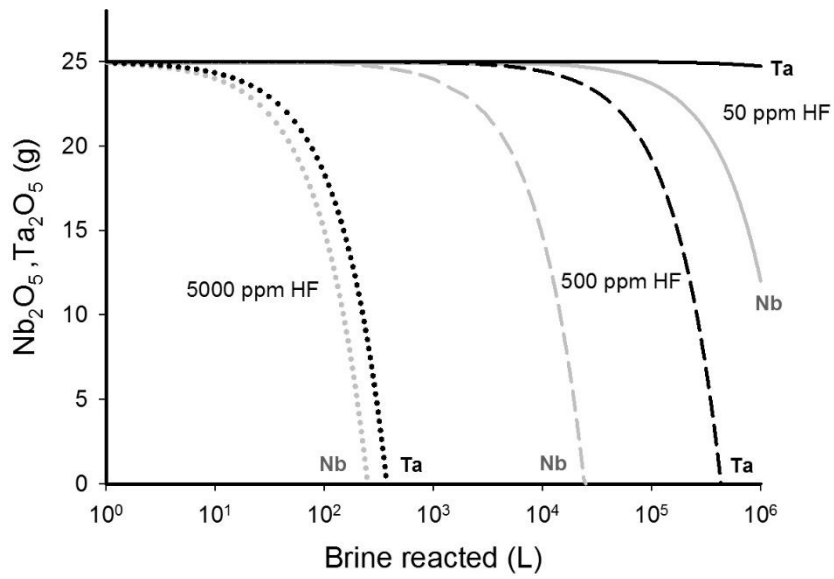
603
604 Figure 5
605



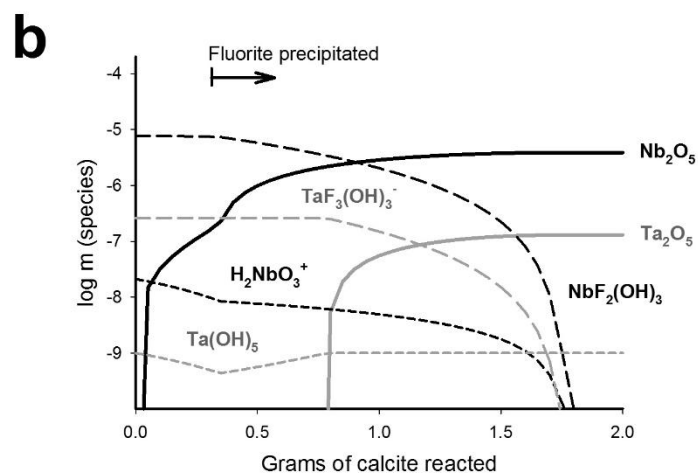
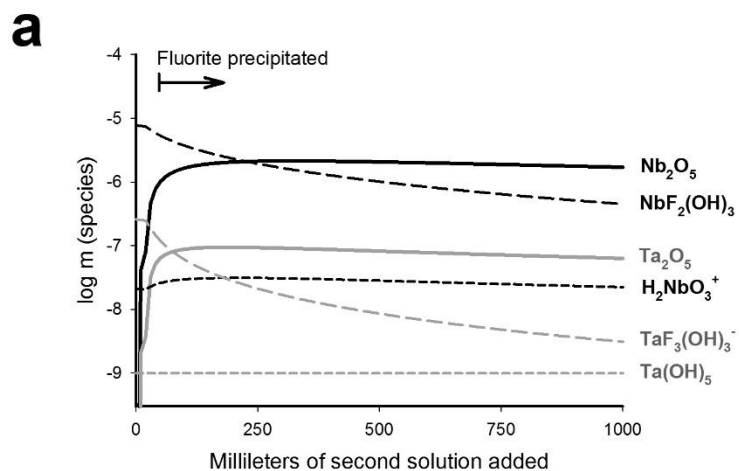
606
607 Figure 6
608



609
610 Figure 7
611
612



613
614 Figure 8
615



616
 617 Figure 9